MABS
2020, VOL. 12, NO. 1, 1–14
https://doi.org/10.1080/19420862.2020.1770018

Taylor & Francis
Taylor & Francis Group

REPORT

OPEN ACCESS Check for updates

Characterization of concurrent target suppression by JNJ-61178104, a bispecific antibody against human tumor necrosis factor and interleukin-17A

Songmao Zheng[a], Fang Shen[b], Brian Jones[b], Damien Fink[a], Brian Geist[a], Ivo Nnane[c], Zhao Zhou[b], Jeff Hall[b], Ravi Malaviya[b], Tatiana Ort[b], and Weirong Wang[c]

[a]Biologics Development Sciences, Janssen Biotherapeutics, Janssen R&D, Spring House, PA, USA; [b]Immunology Discovery, Clinical Pharmacology and Pharmacometrics, Janssen R&D, Spring House, PA, USA; [c]Clinical Pharmacology and Pharmacometrics, Janssen R&D, Spring House, PA, USA

ABSTRACT

Tumor necrosis factor (TNF) and interleukin (IL)-17A are pleiotropic cytokines implicated in the pathogenesis of several autoimmune diseases including rheumatoid arthritis (RA) and psoriatic arthritis (PsA). JNJ-61178104 is a novel human anti-TNF and anti-IL-17A monovalent, bispecific antibody that binds to both human TNF and human IL-17A with high affinities and blocks the binding of TNF and IL-17A to their receptors *in vitro*. JNJ-61178104 also potently neutralizes TNF and IL-17A-mediated downstream effects in multiple cell-based assays. *In vivo*, treatment with JNJ-61178104 resulted in dose-dependent inhibition of cellular influx in a human IL-17A/TNF-induced murine lung neutrophilia model and the inhibitory effects of JNJ-61178104 were more potent than the treatment with bivalent parental anti-TNF or anti-IL-17A antibodies. JNJ-61178104 was shown to engage its targets, TNF and IL-17A, in systemic circulation measured as drug/target complex formation in normal cynomolgus monkeys (cyno). Surprisingly, quantitative target engagement assessment suggested lower apparent *in vivo* target-binding affinities for JNJ-61178104 compared to its bivalent parental antibodies, despite their similar *in vitro* target-binding affinities. The target engagement profiles of JNJ-61178104 in humans were in general agreement with the predicted profiles based on cyno data, suggesting similar differences in the apparent *in vivo* target-binding affinities. These findings show that *in vivo* target engagement of monovalent bispecific antibody does not necessarily recapitulate that of the molar-equivalent dose of its bivalent parental antibody. Our results also offer valuable insights into the understanding of the pharmacokinetics/pharmacodynamics and target engagement of other bispecific biologics against dimeric and/or trimeric soluble targets *in vivo*.

ARTICLE HISTORY
Received 3 January 2020
Revised 27 April 2020
Accepted 6 May 2020

KEYWORDS
bispecific antibody; TNF; IL-17A; target engagement; target-mediated drug disposition; translational modeling

Introduction

Therapeutic biologics targeting inflammatory cytokines have revolutionized the treatment of various autoimmune and inflammatory conditions, including rheumatoid arthritis (RA), inflammatory bowel diseases (IBD), psoriatic arthritis (PsA) and psoriasis (PsO).[1,2] However, these diseases can be mediated by multiple pathogenic processes driven by distinct pro-inflammatory cytokines, such as tumor necrosis factor (TNF) and interleukin (IL)-17A, and treatment with a single inhibitor may lead to inadequate clinical responses.[3,4] Novel biotherapeutics with the potential to neutralize mediators involved in more than one disease may provide opportunities for improved efficacy and enhanced response rates.[5–7]

TNF is a critical pro-inflammatory cytokine produced by both immune cells and nonimmune cells.[8–10] TNF binds to two trimeric transmembrane receptors, TNF receptor 1 (TNFR1) and TNF receptor 2 (TNFR2), and drives the production of other proinflammatory cytokines, expression and activation of adhesion molecules and stimulation of cell growth.[10–12] It is well documented that TNF acts as a prominent inflammatory mediator and plays a key pathogenic role in many rheumatological diseases, including RA, PsA, PsO and gastrointestinal inflammatory conditions such as Crohn's disease (CD) and ulcerative colitis (UC).[10] Five TNF antagonists have been approved for the treatment of RA, including golimumab, a human IgG1 kappa monoclonal antibody (mAb) that specifically binds to human TNF and neutralizes its downstream activities.[13]

IL-17A, a key member of the IL-17 cytokine family, is mainly produced by CD4+ T helper 17 (Th17) cells and several innate-like T-cell populations.[14] IL-17A homodimer binds to heterodimeric receptor complex consisting of IL-17RA and IL-17RC and drives expression of cytokines and chemokines, recruitment and activation of leukocytes, and tissue damage.[15] A rapidly growing body of literature suggests that IL-17A promotes the chronic inflammation underlying the pathophysiology of many autoimmune and inflammatory disorders, including RA.[16] Secukinumab, ixekizumab and brodalumab, which all target the IL-17A pathway, are approved as treatments for various inflammatory diseases.[17] However, blockade of IL-17A alone seems to have limited effects in RA and PsA patients.[18]

Several lines of evidence have suggested that neutralizing TNF and IL-17A concurrently may potentially provide greater clinical benefits compared with neutralizing either cytokine alone.[19–22] In preclinical rodent arthritis models, we and others

CONTACT Weirong Wang wwang83@its.jnj.com 1400 MCKEAN RD, JANSSEN RD, Spring house, PA 19477, USA

have demonstrated that concurrent dosing of anti-TNF and anti-IL17A antibodies is more efficacious in reducing inflammation and protecting against joint damage than individual treatment alone.[4,8,20,21] Anti-TNF treatment was reported to result in an increase of Th17 cell number or IL-17A production in RA patients.[8] In a study of RA patients, TNF and IL-17A mRNA levels in synovial tissue were shown to be synergistically prognostic for joint damage progression.[22] ABT-122, a dual-variable domain immunoglobulin G1 molecule that binds to both TNF and IL-17, has been tested for the treatment of RA and other immune-mediated inflammatory diseases.[23,24] COVA 322, a bispecific TNF/IL-17A-binding FynomAb, had been tested in a Phase 1b/2a study in psoriasis patients.[25]

In this report, we describe the discovery and characterization of JNJ-61178104 (JNJ-8104), a novel anti-TNF and anti-IL-17A bispecific Duobody® antibody developed for the treatment of autoimmune and inflammatory diseases. *In vitro*, JNJ-8104 binds to human TNF and IL-17A with high affinities and neutralizes both cytokines simultaneously. *In vivo*, JNJ-8104 was more effective in preventing neutrophilia induced by human TNF (hTNF) and human IL-17A (HIL-17A) in murine lung than individual anti-TNF or anti-IL-17A mAbs. The safety, tolerability, pharmacokinetics (PK), pharmacodynamics (PD) and immunogenicity of JNJ-8104 were investigated in a first-in-human (FIH) study.[26]

As anti-cytokine mAbs function via the target neutralization, their PD effect is driven by the magnitude and duration of free (unbound) cytokine lowering.[27,28] However, it can be technically challenging to directly measure the reduction of free cytokines, given their low baseline levels, and multiple sources of potential perturbation of the mAb/target binding equilibrium during bioanalysis.[29,30] Mechanism-based mathematical modeling has been extensively used to facilitate the understanding of PK/PD relationships for therapeutic biologics.[31,32] In particular, target-mediated drug disposition (TMDD) models have been applied broadly to describe the interplay between mAbs and their cytokine targets.[30,33-37] Following dosing of mAbs, besides the lowering of the free target due to mAb binding, cytokine target engagement (TE) can also be reflected by a rapid accumulation of the mAb/target complex due to the significant lowering of the target elimination rate after it forms a mAb/target complex.[27,28] A TMDD model that accounts for the *in vivo* kinetics for the mAb, the target and the mAb/target complex can be used to mitigate certain bioanalytical challenges often associated with free target measurement and provide a comprehensive understanding of the PK/TE relationship.[27,28] In order to quantitatively assess TE of JNJ-8104 *in vivo*, multiple cynomolgus monkey (cyno) studies were conducted. A TMDD model was developed to characterize the *in vivo* TNF and IL-17A TE of JNJ-8104 in cynos. The relationship was further examined using simulation approaches in normal healthy human subjects in the FIH study, and the results agreed reasonably well with the observed data.[26]

Results

In vitro binding kinetics of JNJ-8104

To determine the *in vitro* affinity of JNJ-8104 to its targets, recombinant human (rh) or monkey TNF and IL-17A proteins were exposed to immobilized antibodies, and monovalent target-binding kinetics was determined by surface plasmon resonance (SPR). Anti-TNF antibody golimumab and anti-IL-17A antibody CNTO 6785 were included as controls. The results are summarized in Table 1. JNJ-8104 bound to both human and cyno TNF with monovalent affinities that were very similar to golimumab, which was expected because JNJ-8104 possesses the same target-binding antigen-binding fragment (Fab) arm as golimumab. Note that both JNJ-8104 and golimumab bound to human TNF with more than 10-fold higher affinities than to cyno TNF. Both JNJ-8104 and CNTO 6785 bound to human and cyno IL-17A with comparable affinities. Not surprisingly, JNJ-8104 also bound to human and cyno IL-17A with monovalent affinities very similar to CNTO 6785.

In vitro activities of JNJ-8104

Like its parental mAbs, binding of JNJ-8104 inhibited the binding of rhTNF to its receptors TNFR1 (p55) and TNFR2 (p75), and the binding of rhIL-17A to its receptor IL-17RA, in a concentration-dependent manner (data not shown). Moreover, JNJ-8104 inhibited the function of rhTNF and rhIL-17A in a concentration-dependent manner in multiple *in vitro* functional assays (data not shown). Two representative IC_{50} values from an rhTNF-induced WEHI cells cytotoxicity assay and a rhIL17A-induced normal human dermal fibroblasts (NHDFs) growth-regulated oncogene-alpha (GROα) production assay are shown in Table 1. Given each JNJ-8104 molecule has only one arm, but each parental mAb molecule has two arms, to neutralize TNF or IL17A, we estimated that JNJ-8104 would be ~2-fold less potent in cellular neutralization assays. Indeed, JNJ-8104 exhibited 2 ~3-fold higher IC_{50} than the parental mAbs in these two assays. Interestingly, these relatively minor differences in IC_{50} were consistent across multiple *in vitro* functional assays.

The ability of JNJ-8104 to neutralize inflammatory responses mediated by endogenous TNF and IL-17A was tested in a

Table 1. Summary of JNJ-8104, golimumab and CNTO 6785 *in vitro* target-binding kinetics and activities.

Compound	Ligand	Ka (1/Ms)	kd (1/s)	K_D (M)	Compound	Ligand	Readout	IC_{50} (M)
Golimumab	Human TNFα	1.52E+06	4.53E-05	2.98E-11	CNTO 9809	Human TNFα	Cytotoxicity in WEHI cells	6.25E-10
JNJ-8104		1.87E+06	3.72E-05	2.00E-11	JNJ-8104			1.33E-09
CNTO 6785	Human IL-17A	1.55E+06	4.79E-05	3.09E-11	CNTO 4782	Human IL-17A	GROα production in NHDFs	2.57E-11
JNJ-8104		1.38E+06	4.07E-05	3.37E-11	JNJ-8104			6.55E-11
Golimumab	Cyno TNFα	2.11E+05	1.44E-04	6.81E-10	CNTO 9809	Cyno TNFα	Cytotoxicity in WEHI cells	4.39E-09
JNJ-8104		4.70E+05	1.15E-04	2.93E-10	JNJ-8104			1.15E-08
CNTO 6785	Cyno IL-17A	1.29E+06	3.68E-05	2.86E-11	CNTO 4782	Cyno IL-17A	GROα production in NHDFs	3.50E-11
JNJ-8104		1.49E+06	4.12E-05	2.77E-11	JNJ-8104			2.53E-10

co-culture system consisting of human fibroblast-like synovial cells isolated from RA patients (RA-FLS) and *in vitro* primed human T_h1/T_h17 cells. In this co-culture system, TNF and IL-17A were endogenously produced by the activated T cells and RA-FLS. As shown in Figure 1, either anti-TNF or anti-IL-17A parental antibody alone could only partially neutralize the production of IL-6 and GROα, suggesting that both TNF and IL-17A contribute to the inflammatory responses and neutralization of either cytokine alone cannot provide full suppression of the inflammatory responses. In contrast, JNJ-8104 was able to fully inhibit IL-6 and GROα production in the co-culture system in a concentration-dependent manner, with similar potency to the combination of parental bivalent anti-TNF and anti-IL-17A antibodies (Figure 1a,b). This data demonstrated *in vitro* functional potency of JNJ-8104 in inhibiting both TNF and IL-17A simultaneously.

In vivo functional activity of JNJ-8104 in a mouse lung neutrophilia model

Intranasal instillation of a combination of rhTNF and rhIL-17A (0.3 µg each) resulted in significantly increased cellular influx and neutrophilia in bronchoalveolar lavage (BAL) fluid (Figure 2). Compared with that following 10 mg/kg of isotype control, the parental antibodies CNTO 9809 or CNTO 4782 alone demonstrated limited attenuation of the cellular influx in the BAL fluid, while JNJ-8104 prevented cellular influx in a dose-dependent fashion with a near complete ablation at 10 mg/kg (Figure 2). Thus, JNJ-8104 was more efficacious in preventing cellular influx than its parental antibodies alone.

Engagement of endogenous TNF and IL-17A in cynomolgus monkeys

Next, the ability of JNJ-8104 to engage TNF and IL-17A *in vivo* was quantitatively assessed in cynos together with golimumab and CNTO 6785, which shares the same Fab arm as JNJ-8104's parental antibodies CNTO 9809 and CNTO 4782, respectively. First, a single intravenous (IV) bolus dose of either JNJ-8104 (0.3, 1 or 10 mg/kg), golimumab (0.15 or 0.5 mg/kg), or CNTO 6785 (0.15 mg/kg) was administered to the animals (N = 4/group) on Study Day 0. The serum PK profiles of JNJ-8104, golimumab and CNTO 6785 are shown in Figure 3a. The C_{max} of JNJ-8104, lgolimumab and CNTO 6785 was approximately dose-proportional. For JNJ-8104 and golimumab, i.e., mAbs containing at least one anti-TNF arm, there was an apparent acceleration of mAb elimination after Day 7, presumably due to the development of anti-drug antibodies (ADAs). Similar findings with the early onset of ADAs were made with previous studies of golimumab in cynos.[38]

After dosing JNJ-8104 and golimumab, a rapid, dose-dependent increase in serum total TNF was observed (Figure 3b). Surprisingly, the accumulation of total TNF was significantly lower following JNJ-8104 dosing than that following the molar-equivalent dose of the bivalent antibody golimumab. Even following the high 10 mg/kg JNJ-8104 dosing, the accumulation of total TNF was less than that following the 0.5 mg/kg of golimumab. Similarly, a rapid, dose-dependent increase in serum total IL-17A was observed following the dosing of JNJ-8104 and CNTO 6785, and the accumulation of total IL-17A was significantly lower with JNJ-8104 than that with the molar-equivalent dose of CNTO 6785 (Figure 3c).

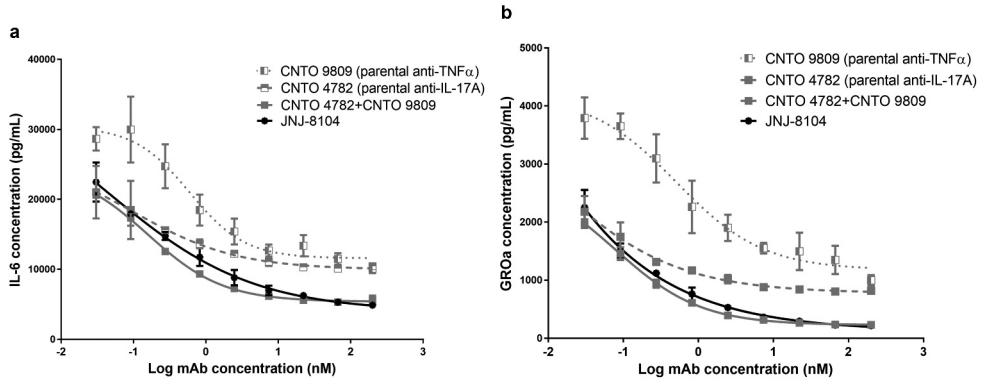

Figure 1. Inhibition of *in vitro* inflammatory responses mediated by endogenous TNF and IL-17A. Human rheumatoid arthritis fibroblast-like synovial cells (RA-FLS) were cocultured with *in vitro* differentiated T_h17/T_h1 cells. Various concentrations of JNJ-8104, CNTO 9809 (parental anti-TNF), CNTO 4782 (parental anti-IL-17A) or equal-molar fixed-ratio combination of CNTO 9809 and CNTO 4782 were incubated with the coculture for 48 hours. Endogenous TNF and IL-17A-mediated production of IL-6 (a) and GROα (b) in the supernatants were measured.

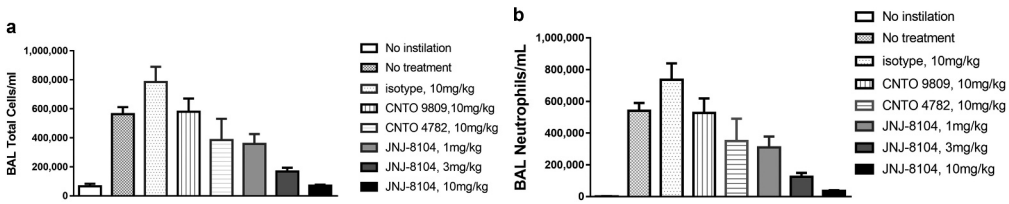

Figure 2. Inhibition of rhTNF- and rhIL-17A-induced Cellular Influx by JNJ-8104 in the Airway Lumen of Mice. Mice were intranasally instilled with rhTNF- and rhIL-17A in combination. After 6 h their lungs were lavaged and total numbers of BAL cells (a) and neutrophils (b) were enumerated as detailed in "Materials & Methods." Mice were injected intraperitoneally with the test mAbs or isotype control18 hours prior to cytokines challenge. Data are represented as mean ± SEM; N = 6–7 mice/group.

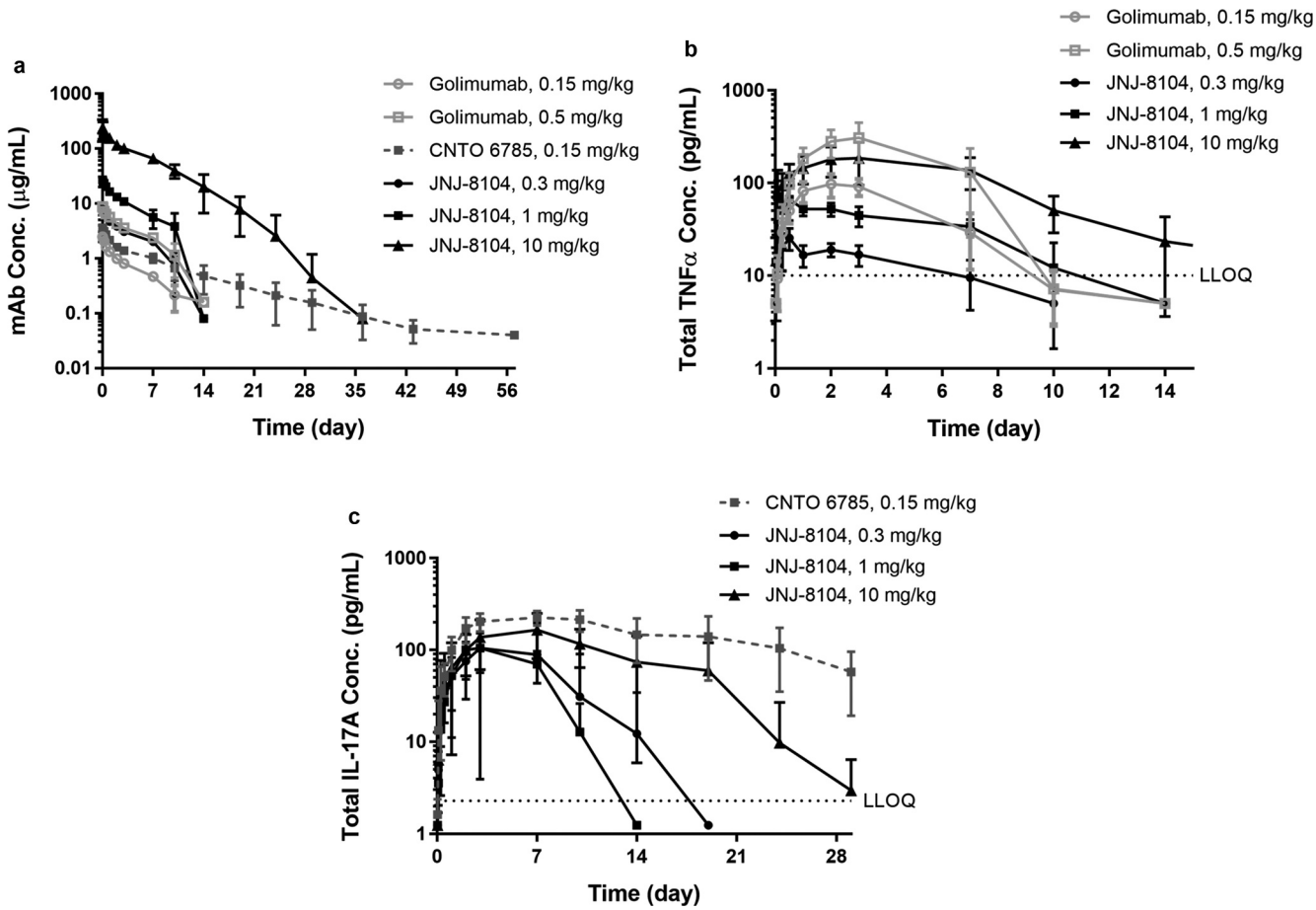

Figure 3. Observed serum concentrations versus time profiles of Total mAb (a), total TNF (b), and Total IL-17A (c) following IV administration of golimumab (parental anti-TNF), CNTO 6785 (anti-IL-17A with identical parental Fab arms) or JNJ-8104 at the specified dose levels in cynomolgus monkeys. Data are represented as mean ± SD.

Application of TMDD modeling to elucidate possible reasons for lower total TNF and IL-17A accumulation following JNJ-8104 administration

Lower accumulation of total TNF and IL-17A can be attributed to decreased formation of the drug/target complex, more rapid elimination of the complex, or both. TMDD-based modeling is commonly used for quantitative characterization of the interaction between a mAb and its soluble cytokine target, and a schematic representation of the model is shown in Figure 4a. Using the modeling terms, the rapid initial increase in the total target concentrations following mAb dosing can be attributed to the significantly lower elimination rate of the mAb/target complex ($k_{el\_complex}$) compared to that of the free cytokine target (k_{deg}). We next investigated what led to the lower accumulation of total TNF and IL-17A following JNJ-8104 dosing.

Using TNF as an example, given the similar PK between JNJ-8104 and golimumab (Figure 3a), k_{el_drug} should be similar between JNJ-8104 and golimumab. The elimination rate constant of free TNF (k_{deg}) is considered independent of mAb treatment, so it should also be the same following JNJ-8104 and golimumab dosing. There are then three possible explanations for the observed lower total TNF accumulation with JNJ-8104 treatment: 1) lower TNF production rate (k_{syn}) following JNJ-8104 dosing than that with golimumab, 2) higher JNJ-8104/TNF complex elimination rate constant ($k_{el\_complex}$) than that of the golimumab/TNF complex, or 3) lower *in vivo* apparent TNF-binding affinity (i.e., higher apparent K_D value) for JNJ-8104 than for golimumab. Among these, the first and third possibilities would lead to less formation of the drug/TNF complex, and the second would lead to more rapid elimination of the complex. These possibilities were examined with additional cyno study results.

Since JNJ-8104 is also expected to suppress the IL-17A target, it is possible that k_{syn} of TNF is lower with IL-17A suppression in cynos. To assess this possibility, accumulation of total TNF in a 3-month GLP toxicology study with weekly 50 mg/kg IV doses of golimumab in the absence or presence of weekly 50 mg/kg IV doses of CNTO 6785, the anti-IL-17A parental mAb, was examined. As shown in Figure 4b, total TNF reached a similar steady-state level (C_{ss}) of ~1,000 pg/mL, with or without CNTO 6785 treatment. Since the IL-17A signaling pathway is expected to be fully suppressed with 14 weekly 50 mg/kg IV doses of CNTO 6785, this result indicated that the k_{syn} of TNF did not change with IL-17A suppression in healthy normal cynos. If the k_{syn} of TNF did not change even with weekly 50 mg/kg doses of CNTO 6785, it is not expected to change significantly with a single, up to 10 mg/kg dose of JNJ-8104.

Next, we examined the second possibility, i.e., whether the mAb/TNF complex degradation rate constant $k_{el\_complex}$ could

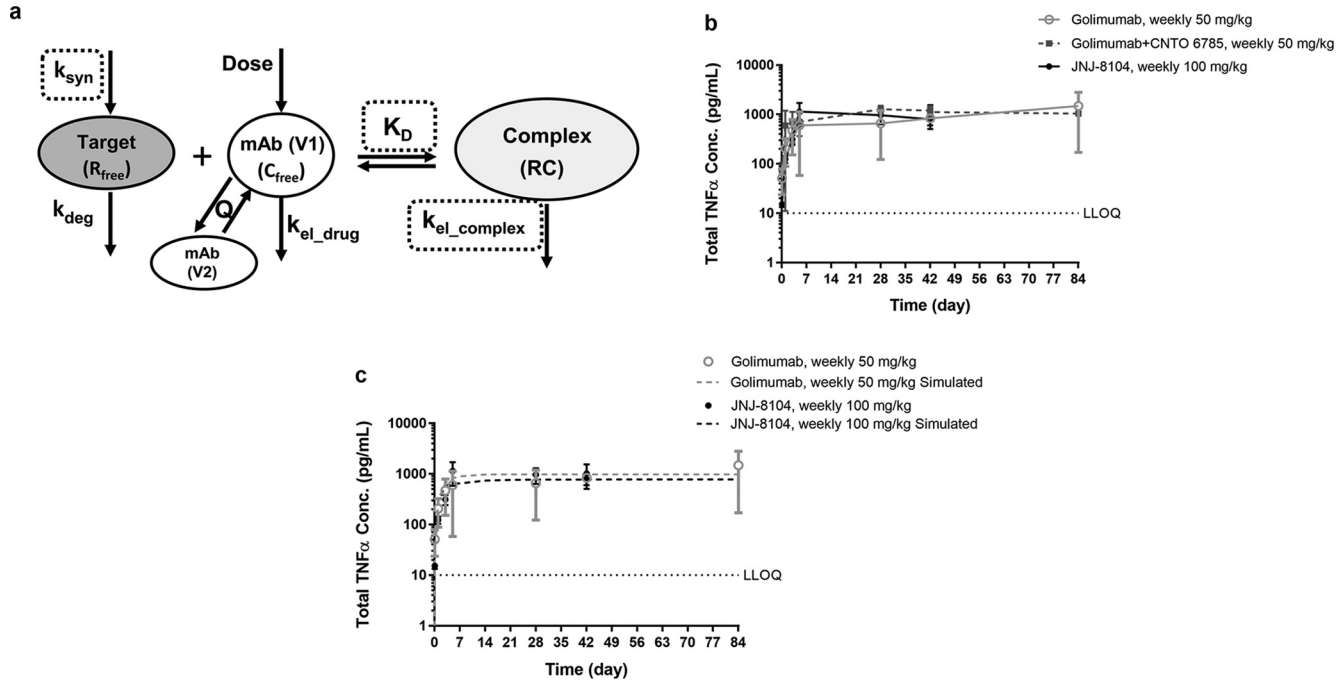

Figure 4. (a) Schematic representation of the TMDD-based PK/TE model. The model parameter names are as defined in Materials and Methods. (b) Observed serum concentrations versus time profiles of Total TNF following 14 weekly high doses of golimumab, golimumab + CNTO 6785 or JNJ-8104 in cynomolgus monkeys. (c) Observed (symbols) and model-predicted (dashed lines) serum concentrations versus time profiles of Total TNF following high doses of golimumab or JNJ-8104 in cynomolgus monkeys. Data are represented as mean ± SD.

be significantly higher with JNJ-8104 than golimumab. In another cyno study, the animals received 14 weekly IV doses of JNJ-8104 at 100 mg/kg. As shown in Figure 4b, the total TNF levels following extremely high doses of JNJ-8104 had reached a similar C_{ss} at ~1,000 pg/mL. In this study, the mAb concentrations reached >1,000 µg/mL, ~6 log higher than the total TNF levels. Under this scenario, the amount of TNF being eliminated as a free target is negligible, and the C_{ss} of total TNF is determined by $k_{syn}/k_{el\_complex}$ (see below for more details). Since k_{syn} of TNF was shown to be similar with or without CNTO 6785 dosing, this result indicated that the mAb/TNF complex elimination rate constants ($k_{el\_complex}$) are also similar for JNJ-8104 and golimumab.

Taken together, these results suggested that the third possibility, i.e., JNJ-8104 binds to endogenous cyno TNF with different apparent affinities than golimumab, is the most likely explanation for the lower total TNF accumulation. This was unanticipated because JNJ-8104 bears the same TNF-binding Fab arm as golimumab, and *in vitro* SPR had shown that they were of similar monovalent binding affinities to both monkey and human TNF (Table 1). To further assess this possibility, we evaluated whether a single different apparent *in vivo* K_D value can quantitatively account for the observed TNF and IL-17A TE data across all dose groups using a TMDD model.

Development of a TMDD model for quantitative assessment of TNF and IL-17A TE in cynomolgus monkeys

TMDD model for TNF

Only PK, total TNF and the baseline TNF from the free TNF assay were used for TNF PK/TE model development. We also attempted to measure the free (i.e., free from mAb binding) TNF levels following mAb dosing, but the results were not usable due to the low TNF baseline in healthy normal cynos. The baseline TNF levels can only be quantified with the free TNF assay, which has a lower limit of quantification (LLOQ) at 0.075 pg/mL. Among the 20 cynos administered JNJ-8104 (0.3, 1 or 10 mg/kg) and golimumab (0.15 or 0.5 mg/kg), their pre-dose TNF baseline values were <0.075 pg/mL for 6 animals, between 0.075 and 1 pg/mL for 10 animals, and >1 (1.2–1.8) pg/mL for 4 animals.

Due to the lack of free TNF data post-dosing, we estimated and fixed a few key model parameters. First, the target production rate constant (k_{syn}) of TNF was estimated from the fastest initial rising slope of the total target profiles. Following mAb treatment, the initial fast rising of the total TNF is due to the dramatic difference in elimination rate constants from that of the free TNF (k_{deg}, usually in minutes for a cytokine) to the mAb/TNF complex ($k_{el\_complex}$, usually in days or weeks). The rate of this initial total TNF level rise is limited by k_{syn}; therefore, it can be estimated from the fastest initial rising slope of the total TNF profiles. With JNJ-8104 treatment, the slope for the total TNF profile (at 50 and 100 mg/kg) was approximately 365 pg/mL/day (k_{syn}). In addition, the TNF baseline was fixed at the observed mean values from all JNJ-8104- and golimumab-treated animals (N = 14; ≈ 0.61 ± 0.30 pg/mL or 0.012 ± 0.005 pM). This value was within twofold of literature reported median values in RA patients.[39] Free TNF elimination rate constant (k_{deg}) was assumed to be the same for all animals and estimated to be ≈ 596 day^{-1}, using $k_{deg} = k_{syn}$/TNF baseline.

The kinetics of the total target concentration (R_{tot}) can be described by Equation (1):

$$\frac{dR_{tot}}{dt} = k_{syn} - k_{deg} \times R_{free} - k_{el\_complex} \times RC \quad (1)$$

When R_{tot} reaches steady state (plateau), $\frac{dR_{tot}}{dt} = 0$, i.e., the right side of Equation (1) equals zero. The highest complex concentration (RC) can be reached when $k_{deg} \times R_{free}$ approaches 0, i.e., R_{free} becomes infinitely low when the antibody dose is extremely high. In this situation, $k_{syn} - k_{el\_complex} \times C_{ss\_complex} = 0$, and therefore $C_{ss\_complex} = k_{syn}/k_{el\_complex}$.

Following JNJ-8104 dosing at 100 mg/kg, the $C_{ss\_complex8104}$ is ≈ 1000 pg/mL, and the $k_{el\_complex8104}$ can be estimated as 365 (pg/mL/day)/1000 (pg/mL) = 0.365 (day^{-1}), within twofold of the calculated mAb elimination rate constant ($k_{el\_JNJ\text{-}8104}$) (≈ 0.21 day^{-1}).

Following golimumab dosing at 50 mg/kg, the $C_{ss\_complex148}$ is ≈ 1000 pg/mL and the rising slope for the total TNF profile is similar to that with 100 mg/kg JNJ-8104 treatment (Figure 4b). Therefore, the elimination rate constant of golimumab-TNF complex ($k_{el\_complex148}$) was fixed at the same value as $k_{el\_complex8104}$ (≈ 0.365 day^{-1}). This value was within twofold of the calculated mAb elimination rate constant of golimumab ($k_{el\_CNTO148)}$ (≈ 0.22 day^{-1}).

The *in vivo* apparent K_D in the TMDD model was estimated by fitting the observed total TNF data for JNJ-8104 and golimumab separately (Figure 5a,b). For JNJ-8104, the model was able to simultaneously characterize the cyno total TNF data reasonably well across the 0.3–10 mg/kg dose range. For 0.3 mg/kg, the mean model prediction was within twofold of the observed mean throughout day 7, and within 1.5-fold for 1 mg/kg and 10 mg/kg across the sampling time points. For golimumab, the model-predicted mean total TNF was within twofold of the observed mean for 0.5 mg/kg and within 2.6-fold for 0.15 mg/kg. In contrast to their similar *in vitro* affinities, the *in vivo* apparent K_D was estimated to be 65.7 pM for golimumab and 1,610 pM for JNJ-8104 (Table 2). Overall, the *in vivo* apparent affinity for golimumab to cyno TNF was ~25-fold higher than JNJ-8104, and this difference in apparent *in vivo* K_D explains the observed differences in total TNF profiles across all dose groups for golimumab and JNJ-8104.

Quantitative assessment of IL-17A TE in cynomolgus monkeys

Unlike free TNF results, the free IL-17A assay had an LLOQ of 0.5 pg/mL and the free IL-17A data following JNJ-8104 treatment in cynos showed apparent dose-response (i.e., 0.3, 1, 10 mg/kg) by visual inspection. Therefore, the free IL-17A data were used together with total IL-17A and JNJ-8104 PK results for PK/TE model development, using a similar quasi-equilibrium TMDD model with IL-17A target-specific parameters.

Unlike mAbs targeting TNF, the IL-17A molecule CNTO 6785 exhibited no apparent acceleration of elimination at > Day 7 time points, following a single IV dose at 0.15 mg/kg in cynos. Therefore, the PK of CNTO 6785, as well as free and total IL-17A data following CNTO 6785 administration, were first used for model development and estimation of IL-17A-specific model parameters. IL-17A baseline level in the PK/TE model was fixed at the observed mean free baseline in cynos (≈ 1.36 ± 0.69 pg/mL or 0.039 ± 0.02 pM, N =10). The rest of the model parameters were estimated.

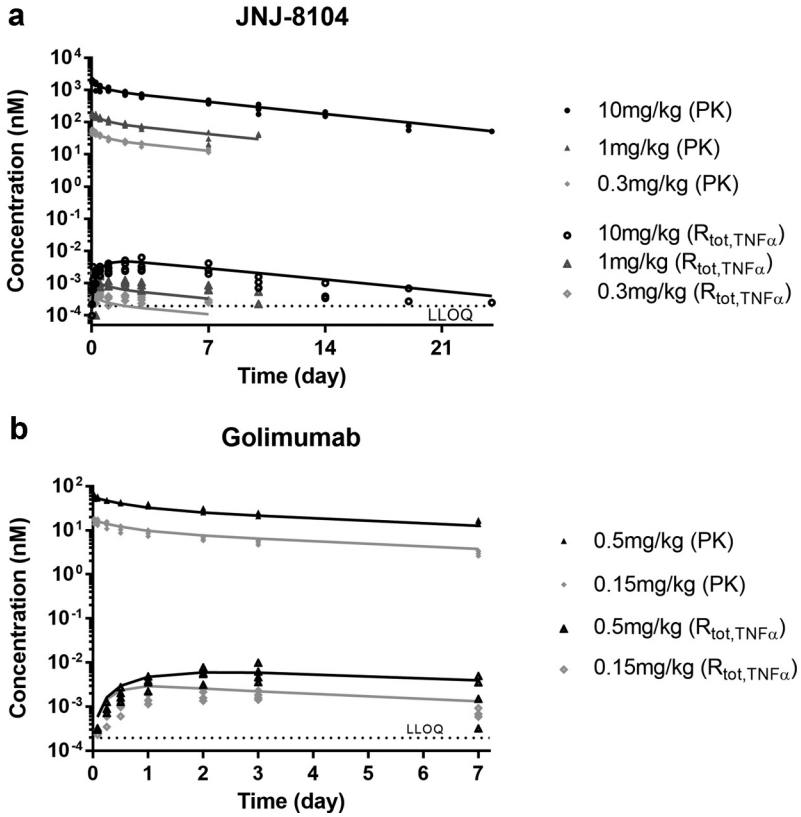

Figure 5. PK/TE model fitting of PK and Total TNF profiles following IV administration of JNJ-8104 (a) and golimumab (b) in cynomolgus monkeys. Symbols = Observed individual data; Lines = Mean model prediction.

Table 2. Estimated JNJ-8104, CNTO148 and CNTO 6785 cynomolgus monkey PK/TE model parameters (mean, residual standard error%) and predicted human parameters.

Parameter (unit)	JNJ-8104 Human, predicted (observed human PK)	JNJ-8104 Human, predicted (allometric scaling)	JNJ-8104 Cyno, estimated	Golimumab Cyno, estimated	CNTO 6785 Cyno, estimated
CL (L/day/kg)	0.00549	0.0048 *	0.0077 (4%)	0.0131 (10%)	0.0072 (14%)
V_1 (L/kg)	0.0464	0.0375 *	0.0375 (5%)	0.0588 (4%)	0.0405 (6%)
V_2 (L/kg)	0.0341	0.0217 *	0.0217 (9%)	0.0342 (9%)	0.0302 (5%)
Q (L/day/kg)	0.00598	0.0140 *	0.0224 (11%)	0.0353 (11%)	0.023 (9%)
TNFα					
k_{deg} (1/day)	271.18 *	271.18 *	596 ●	596 ●	
Baseline (pg/mL)	0.9^^	0.9^^	0.612 ^	0.612 ^	
$k_{el\_complex}$ (1/day)	0.12	0.17*	0.365 ●	0.365 ●	
K_D (pM)	1610	1610	1610 (10%)	65.7 (10%)	
IL-17A					
k_{deg} (1/day)	45.50 *	45.50 *	100 #		100 (31%)
Baseline (pg/mL)	1.365^^^	1.365^^^	0.763 (29%)		1.365 ^
$k_{el\_complex}$ (1/day)	0.12	0.14 *	0.317 (25%)		0.504 (39%)
K_D (pM)	254	254	254 (21%)		38.9 (41%)

The PK data points under apparent impact of ADA were excluded for estimating human PK parameters based on JNJ-61178104 observed PK in the FIH study.
$k_{el\_complex}$ was based on the estimated human PK parameters assuming that $k_{el\_complex}$ for both targets was the same as the elimination rate constant of JNJ-8104 (e.g., calculated as CL/V_1).
*Scaled from JNJ-8104 cyno parameters using BW-based allometric scaling with fixed exponents.
Θ fixed at the estimated parameter values based on JNJ-8104 cyno model fitting.
^^ fixed at the reported population median value for TNFα baseline in RA patients.[40]
^^^ assumed to be the same as cynos and fixed at the observed mean IL-17A baseline in cynos
● fixed based on mathematical derivations using observed data, see section "TMDD model for TNFα" for details.
^ fixed at the observed mean baseline levels for TNFα or IL-17A in cynos
# fixed at the estimated parameter value based on CNTO 6785 cyno model fitting.

The developed PK/TE model (Figure 4a) adequately characterized the PK, total IL-17A and free IL-17A following CNTO 6785 dosing (Figure 6a). The PK/TE model parameters are shown in Table 2. The estimated k_{deg} of IL-17A (≈ 100 day^{-1}) was then fixed for the PK/TE model fitting following JNJ-8104 dosing. JNJ-8104 PK parameters were also fixed to the estimated values from JNJ-8104/TNF PK/TE model. The rest of the model parameters were then estimated.

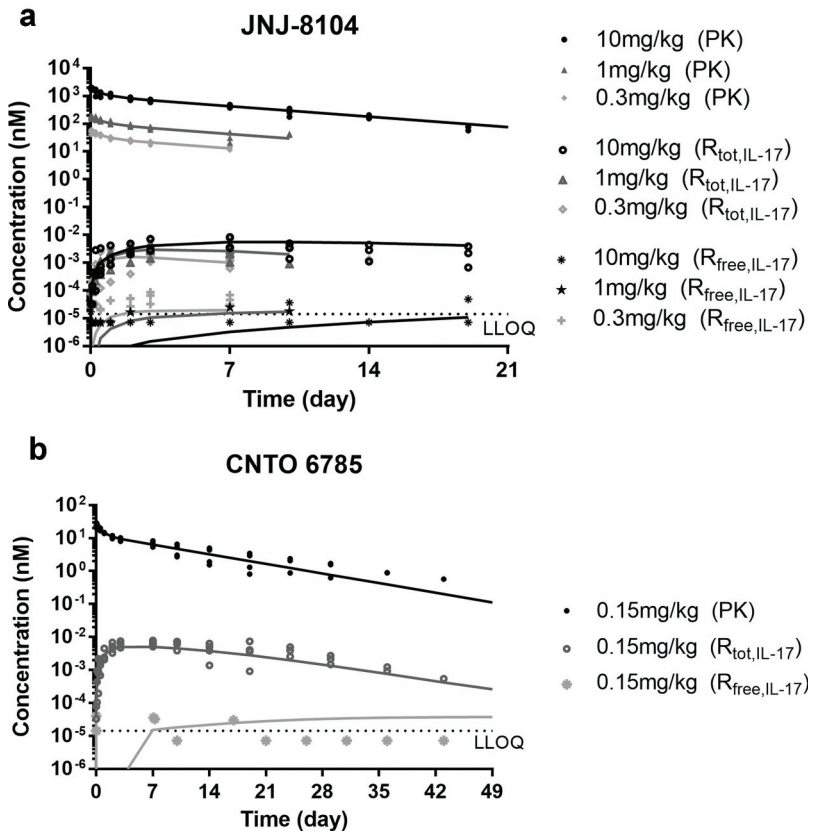

Figure 6. PK/TE model fitting of PK, total IL-17A and Free IL-17A profiles following IV administration of JNJ-8104 (a) and CNTO 6785 (b) in cynomolgus monkeys. Symbols = Observed individual data; Lines = Mean model prediction.

As shown in Figure 6b, the developed model adequately characterized the JNJ-8104 PK, total IL-17A and free IL-17A profiles across all dose groups. The estimated IL-17A baseline (0.763 pg/mL) was within twofold of the observed mean free IL-17A baseline in cynos. The estimated $k_{el\_complex}$ for JNJ-8104/IL-17A complex was within twofold of that estimated for CNTO 6785/IL-17A. Like TNF, the apparent *in vivo* K_D of JNJ-8104 to IL-17A was estimated to be ~254 pM (Table 2), about ninefold higher than the *in vitro* K_D against cyno IL-17A (27.7 pM) determined by SPR and purified protein, while the estimated apparent *in vivo* K_D for CNTO 6785 was ~38.9 pM, similar to the *in vitro* K_D against cyno IL-17A (28.6 pM) determined by SPR.

Taken together, the modeling results for both TNF and IL-17A suggested that a different *in vivo* apparent K_D value can quantitatively account for the observed differences in total TNF/IL-17A profiles between JNJ-8104 and its parental antibodies across the dose ranges examined, suggesting that JNJ-0841 binds to TNF and IL-17A with different *in vivo* K_D compared to its parental antibodies.

TNF and IL-17A TE following JNJ-8104 dosing in humans

To understand the ability of JNJ-8104 to engage TNF and IL-17A in humans, PK and TE samples were collected from JNJ-8104 FIH study in normal healthy subjects.[26] The observed total TNF, total IL-17A, and serum PK profiles in humans were shown in Figures 7 and 8, respectively. The serum total TNF and IL-17A levels were below the LLOQ of 10 pg/mL at baseline and throughout the treatment period in all placebo subjects. Following JNJ-8104 dosing, the increases in mean serum total TNF and IL-17A concentrations were apparent at 2 hours post-dose and reached a maximum of ~100 pg/mL for

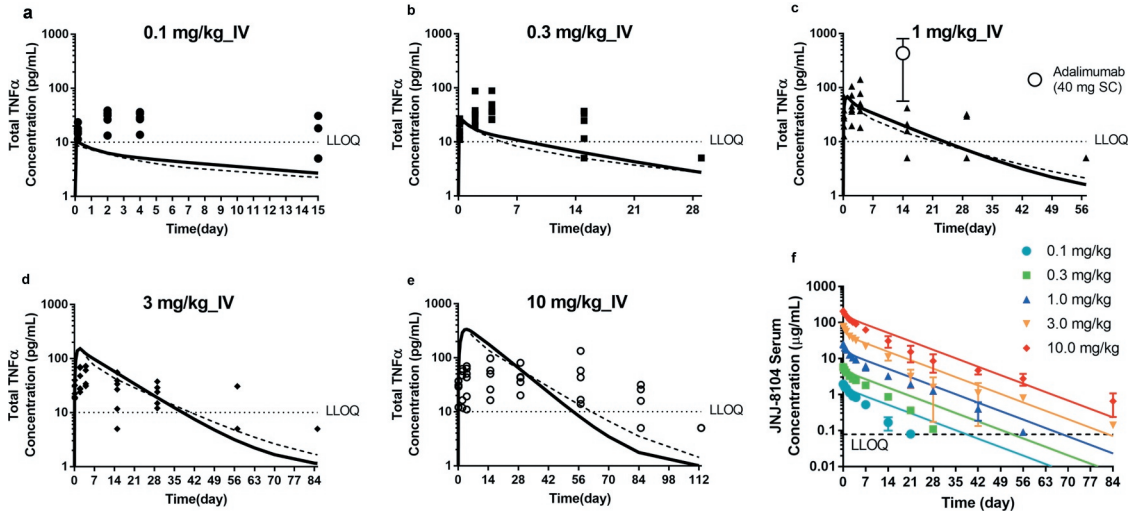

Figure 7. Comparison of observed and model-predicted Total TNF profiles (a–e) and serum drug concentrations (f) following a single IV administration of JNJ-8104 at 0.1, 0.3, 1, 3 and 10 mg/kg in normal human subjects. Symbols = Observed individual data; For A-E: Solid lines = Mean model prediction based on cyno PK/TE model parameters and allometric scaling for human PK; Dotted lines = Mean model prediction based on estimated JNJ-8104 human PK parameters from FIH data with cyno-based *in vivo KD*. The observed mean (SD) concentrations of Total TNF at week 2 trough following 40 mg q2 w SC doses of adalimumab are also shown in Figure 7c. In figure 7f, the colored lines represent the simulated human PK based on allometric scaling from cyno only.

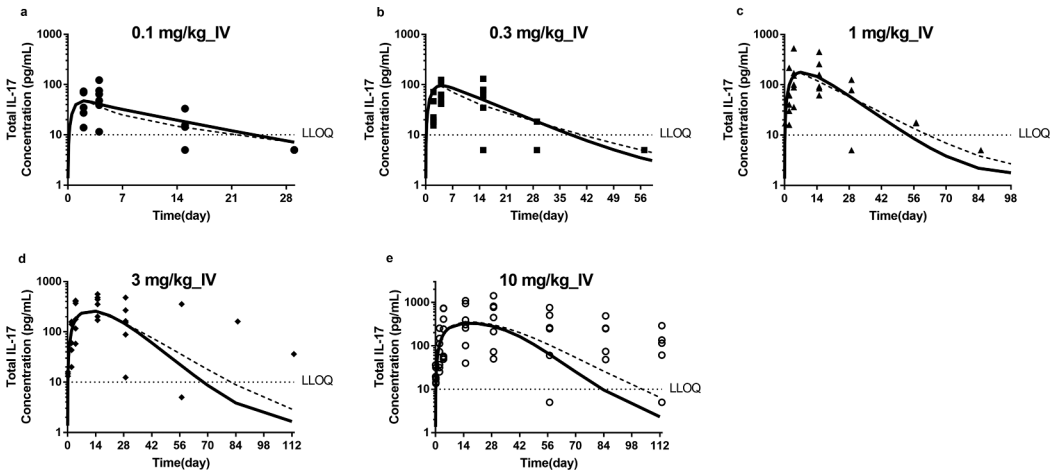

Figure 8. Comparison of observed and model-predicted Total IL-17A profiles following a single IV administration of JNJ-8104 at 0.1, 0.3, 1, 3 and 10 mg/kg (a–e) normal human subjects. Symbols = Observed individual data; Solid lines = Mean model prediction based on cyno PK/TE model parameters and allometric scaling for human PK; Dotted lines = Mean model prediction based on estimated JNJ-8104 human PK parameters from FIH data with cyno-based *in vivo KD*.

total TNF and ~1,000 pg/mL for total IL-17A around Days 2 and 3, and then declined with JNJ-8104 concentrations in a dose-dependent manner.

Since no TNF or IL-17A TE was assessed when golimumab or CNTO 6785 were studied in humans, we cannot compare the total TNF and total IL-17A profiles following JNJ-8104 dosing directly to those of its parental antibodies. Fortunately, accumulation of total TNF was measured at week 2 trough following 40 mg, once every 2 weeks (Q2 W), subcutaneous (SC) dose of adalimumab (Humira®), a bivalent antibody that binds to human TNF with affinities similar to that of golimumab,[41] (internal data from study NCT02019472, ClinicalTrials.gov identifier, CNTO136ARA3005). Assuming average SC bioavailability (65%) and body weight (80 kg), the 40 mg SC dose corresponds to approximately 0.32 mg/kg IV dose of adalimumab, or 0.64 mg/kg molar-equivalent dose of monovalent anti-TNF antibody. The observed total TNF profiles following 40 mg SC dose of adalimumab at Week 2 trough were also presented in Figure 7c, together with that following 1.0 mg/kg IV dose of JNJ-8104. We found that the total TNF accumulation following approximate molar-equivalent adalimumab dosing was ~20-fold higher compared to JNJ-8104, indicating that JNJ-8104 could not engage TNF as effectively as a bivalent antibody with similar *in vitro* monovalent target-binding affinity.

The observed total TNF, total IL-17A and serum PK profiles in humans were also overlaid directly with the model-simulated profiles using cyno-based PK/TE parameters and allometric scaling (Figure 7a–e, 8, and 7f, respectively). Considering that the predictions were conducted entirely *a priori*, the model simulation results reasonably captured the overall trend of total TNF, total IL-17A and serum PK profiles, suggesting JNJ-8104 also engaged both TNF and IL-17A in normal human subjects differently comparing to their bivalent parental antibodies as observed in cynos. It is interesting to note that unlike in cyno, the model appeared to have difficulty simultaneously capture the total TNF dynamics across the 0.1–10 mg/kg dose range. When the predicted JNJ-8104 human PK parameters were replaced with ones estimated from the observed FIH PK data, it only slightly improved the prediction (Figures 7a–e and 8, dotted lines), suggesting that the discrepancy was not due to inaccurate prediction of JNJ-8104 human PK. The exact mechanism of this non-dose proportional total target, especially TNF, dynamics is unknown, but it may be related to some concentration-dependent drug/target complex formation (e.g., through avidity effect) and/or elimination (e.g., differences in the stoichiometry of JNJ-8104/TNFα complex, concentration-dependent involvement of other soluble TNF receptor or cofactors in the complex, and their associated differential elimination rate constants, or non-constant TNF production rate). These mechanisms, including potential inter-species differences, could be an interesting topic for future investigation.

Discussion

JNJ-8104 is a monovalent, bispecific antibody that binds to both human TNF and IL-17A. The target-binding arms of JNJ-8104 are the same as its anti-TNF and anti-IL-17A parental antibodies, respectively, and *in vitro* SPR assays showed that the monovalent target-binding affinities of JNJ-8104 to both targets were similar to its parental antibodies (Table 1). JNJ-8104 was also shown to inhibit TNF – or IL-17A-mediated downstream effects in cellular assays in a dose-dependent manner, though its potency was found to be consistently two to threefold lower than their parental antibodies across multiple assays. In the TNF – and IL-17A-mediated mouse lung neutrophilia model, JNJ-8104 demonstrated its ability to fully neutralize both TNF and IL-17A *in vivo*. However, when JNJ-8104 was dosed in healthy normal cynos, the accumulation of drug/target complex was found to be significantly lower than that following the molar-equivalent dose of its corresponding bivalent parental antibodies. Quantitative TE assessment suggested that the differences in drug/target complex accumulation were most likely explained by lower apparent *in vivo* target-binding affinities of JNJ-8104 than its bivalent parental antibodies, not a change in the target production rate nor a change in the elimination rate constant of drug/target complex. The differences in total target accumulation were not related to the effect of ADA either because the differences in the accumulation of total target were already apparent 2 hours after the animals received their first dose of mAbs, and reached the maximum ~2–3 days after dosing, before any ADA can be developed. Similar findings were made in the FIH study of JNJ-8104, suggesting it also binds to human TNF and IL-17A with lower apparent affinities *in vivo*.

It is unexpected that JNJ-8104 could have 10- to 20-fold lower apparent *in vivo* target-binding affinities than its parental antibodies when all *in vitro* measurements suggested JNJ-8104 had a similar affinity and potency as its parental antibodies. Nevertheless, the collective cyno study results and analysis suggested that this is the most logical explanation for the observed lower total target accumulation. One possible explanation for this discrepancy between *in vitro* and *in vivo* assessment is related to the differential binding characteristics of monovalent and bivalent antibodies when binding to extremely low-abundance (e.g., <0.1 pM) dimeric (e.g., IL-17A) or trimeric (e.g., TNF) targets. Binding affinity describes the strength of the binding interaction between two molecules, and it is supposed to be concentration-independent. It is also not supposed to be affected by avidity if the target interaction with each binding site is entirely independent. However, when the *in vivo* physiological system is not in rapid equilibrium, i.e., when the target molecule is dimeric or trimeric, in extremely low abundance and subject to rapid elimination from the system, it is possible that the apparent affinity is higher for a bivalent antibody because the target molecules dissociated from the first binding site are easier to be re-captured if there is a second binding site in close proximity, thus leading to a lower apparent dissociation rate. This benefit of bivalent binding is likely not apparent under *in vitro* experimental conditions, where the target concentrations are much higher and the system is in rapid equilibrium. Along this line of reasoning, it is interesting to note that all the *in vitro* experimental systems in which JNJ-8104 exhibited similar activities compared with its parental antibodies used non-physiologically high concentrations of TNF or IL-17A.

Admittedly, though the apparent *in vivo* affinity change is a likely logical explanation for the observed differences in total TNF and total IL-17 accumulation in *vivo*, other possible explanations cannot be excluded and the exact cause of these differential binding characteristics remains to be elucidated.

A bispecific drug targeting two targets involved in disease pathways may have advantages over a combination of two drugs from both logistical and cost perspectives. Concurrent inhibition of TNF and IL-17A remains a promising therapeutic opportunity as the next-generation treatment for RA and other autoimmune diseases.[4–7] Co-inhibition of TNF/IL-17A pathway had shown superior efficacy in blocking cytokine and chemokine responses *in vitro* and in preclinical RA models.[4] Of note, even though our results suggested that the production of TNF did not change significantly with IL-17A suppression in normal cynos, this does not mean the production of TNF would not change with IL-17A inhibition, or *vice versa*, under inflammatory disease conditions.

Although the reason for the apparent inferior JNJ-8104 *in vivo* target engagement is not fully understood and its impact on the ability of JNJ-8104 to modulate disease state remains to be seen, our study provides valuable insights into the design of biologics against dimeric or trimeric soluble targets. It also highlighted that quantitative target engagement assessment is an important consideration when examining the mechanism of actions for biotherapeutics directed against soluble targets. Although engaging the target alone does not guarantee efficacy, it is a quantifiable first-step for a drug to elicit its downstream pharmacological effects. For mAbs directed against cytokines, their therapeutic efficacy is expected to be driven by the magnitude and duration of free cytokine suppression. Given the low physiological levels of most cytokines, particularly in healthy conditions, direct measurement of the lowering of free cytokines following drug treatment can be challenging. In our study, we were unable to generate meaningful-free TNF measurements in cynos, and neither free TNF nor free IL-17A in humans. Mechanism-based TMDD modeling can be used to facilitate quantitative assessment of the interplay between drug and free/bound target and corresponding target modulation. As pointed out in published reviews, the TMDD model parameter identifiability can be a challenge when only the total drug and total target concentrations are available, unless a good estimate of the *in vivo* K_D or k_{syn}/k_{deg} values can be generated.[27,28] In the absence of free TNF data, we first estimated k_{syn} of TNFα from the fastest initial rising slope of the total target profiles and subsequently k_{deg} from the TNF baseline. The model-estimated apparent *in vivo* K_D for golimumab was 65.7 pM, ~10-fold lower than the *in vitro* K_D determined by SPR (681 pM). In contrast, the *in vivo* apparent K_D of JNJ-8104 was estimated to be 1,610 pM, ~fivefold higher than the *in vitro* K_D (293 pM). Overall, the apparent *in vivo* K_D for golimumab was ~25-fold lower than JNJ-8104, indicating substantial differences in endogenous TNF binding between molar-equivalent doses of monovalent and bivalent anti-TNF antibodies.

The model-estimated elimination rate constant for free TNF is 596 day^{-1} indicating the half-life of endogenous TNF was ~1.7 minutes in monkeys and the allometrically scaled half-life of endogenous TNF in human was ~3.7 min. This is considerably lower than some of the reported plasma half-life of rhTNF in rats.[42,43] While there is always uncertainty in model parameter estimates, it is important to note that all studies that studied the kinetics of rhTNF were conducted at concentration ranges substantially higher than the physiologically relevant levels. The saturable TNF receptor-mediated binding and disposition have been suggested to be a dominant elimination pathway for TNF.[42] It is interesting to note that the study using the lowest rhTNF dose (5 μg/kg) reported the lowest plasma half-life (~6 min),[42] compared to other studies that reported half-lives of 30–60 min.[42] The systemic half-life of IL-17 is considered to be short and IL-17 is difficult to detect in serum and bodily fluids.[44] The model-estimated half-life for endogenous IL-17A was ~10 min in monkeys based on estimated elimination rate constant of 100 day^{-1} and the allometrically scaled half-life of endogenous IL-17A in human was ~22 min.

Target engagement assessment could perhaps have been valuable in the case of ABT-122, a bispecific Dual-Variable Domain Immunoglobulin (DVD-Ig) targeting TNF and IL-17A being developed for autoimmune diseases.[23,24] ABT-122 has demonstrated dose- and time-dependent efficacy in Phase 2 studies in RA and PsA patients.[23,24] However, a recent exposure-response analysis suggested that at comparable molar exposures, there was no clear differentiation of efficacy between ABT-122 and adalimumab, the anti-TNF parental antibody of ABT-122, and the authors concluded that there was no incremental benefit of inhibiting the IL-17A pathway in the presence of TNF inhibition.[45] A potential caveat of this conclusion is that target engagement assessment may not have been taken into account (or published). Therefore, it was unclear whether comparable molar exposures of ABT-122 and adalimumab actually led to comparable levels of TNF target engagement *in vivo*, and thus leaves uncertainty about the assessment of the contribution of IL-17A pathway inhibition.

In summary, drug effects *in vivo* can be more complex than anticipated, especially for newer classes of biotherapeutics such as bispecific antibodies. Our experiences demonstrated the value of target engagement assessment *in vivo*, and the utility of quantitative modeling in developing such drugs, including aiding the design of proper molecular formats based on target properties, and in predicting human PK/TE using preclinical data.

Materials & methods

JNJ-61178104 (JNJ-8104) and its parental antibodies

JNJ-8104 is a fully human bispecific antibody against TNF and IL-17A generated from two IgG1 kappa antibodies: parental anti-TNF antibody, CNTO 9809, which shares the complementarity-determining regions (CDRs) with golimumab,[46] but carries a point mutation in the Fc region to facilitate the production of Duobody®; and parental anti-IL17A antibody, CNTO 4782, which shares the CDR with CNTO 6785 and carries another point mutation in the Fc region to facilitate the production of Duobody®.[47] The bispecific JNJ-8104 Duobody® is generated from these parental antibodies CNTO 9809 and CNTO 4782 (generated by Janssen R&D, Spring

House, PA, USA) using Fab arm exchange technology developed by Genmab (Copenhagen, Denmark).[48] Golimumab and CNTO 6785 were used in cyno studies as the bivalent parental antibodies of JNJ-8104 to study TNF and IL-17A target binding. The recombinant human and cyno TNF and IL-17A proteins were also generated at Janssen R&D (Spring House, PA).

In vitro target-binding kinetics

The monovalent binding kinetics for JNJ-8104 and its parental antibodies to human and cyno TNF and IL-17A were measured by SPR using purified recombinant proteins on a Biacore 3000 (GE Healthcare Life Sciences, Pittsburgh, PA). In order to determine the monovalent binding affinity for all antibodies, each test antibody (75 ~200 response unit (RU)) was first captured by goat anti-human IgG Fc (16,000 RU, Jackson labs #109-005-098) that had been coupled to sensor surface (CM5 chip, Biacore #BR-1000-14). Purified recombinant human or cyno TNF or IL-17A proteins were formulated in Dulbecco's phosphate-buffered saline (PBS; Invitrogen #14190) with 100 µg/mL bovine serum albumin (BSA; Jackson ImmunoResearch #001-000-161) and 0.01% surfactant P20 (Biacore #BR-1000-54) at 20°C and diluted into 4 different concentrations. Diluted TNF or IL-17A proteins were injected and flowed over the captured test antibody to measure the binding kinetics. The association was monitored for 3 minutes (150 µL, 50 µL/min). The dissociation was monitored for 20 minutes to 2 hours depending on the off-rate. Short-and-long dissociation methods[49] were applied to enhance the estimation of the affinity of tight binders with off-rate values less than 10^{-5} regenerations of the sensor surface was performed with a 9-s injection of 100 mM H_3PO_4. The collected data were processed and fitted to a 1:1 Langmuir binding model to determine the k_{on} and k_{off} rates.

TNF-induced cytotoxicity in WEHI cells

Mus musculus fibrosarcoma WEHI-164 cells (ATCC CRL-1751, Manassas, VA) were seeded into 96-well microtiter plates (5×10^4 cells in 50 µL/well) and incubated overnight at 37°C. Serial dilutions of each mAb were pre-incubated with 100 pg/mL of recombinant human TNF or 100 pg/mL recombinant cyno TNF in medium containing 1 ug/mL of actinomycin D, followed by overnight incubation with the cells. Cell viability was read by Celltiter Glo (Promega, Madison, WI). IC_{50} values were determined by non-linear regression using GraphPad Prism software Version 7.00 (GraphPad Software, San Diego, CA).

IL-17A induced GROα production in NHDFs

Normal Human Dermal Fibroblasts (NHDF) cells (Lonza, Morristown, NJ) were seeded into a 96-well flat-bottom tissue culture plate at 5,000 cells per well in FGM-2 medium (Lonza) and incubated overnight (37°at 5% CO_2). Following incubation, 10 ng/mL of recombinant human IL-17A (Janssen R&D) or 10 ng/mL of recombinant cyno IL17A (Janssen R&D) was pre-incubated with serial dilution (30–0.0015 µg/mL) of antibodies and then apply to NHDFs. Cells were incubated for 24 h (37°, 5% CO_2) in the presence of 10 ng/mL of recombinant human TNF or 10 ng/mL of recombinant cyno TNF and culture supernatants were collected and assayed by ELISA for human or cyno GROα (R&D Systems, Minneapolis, MN). IC_{50} values were determined by non-linear regression using GraphPad Prism.

JNJ-8104 activity in an RA-FLS and T_h17/T_h1 cell co-culture system

Human rheumatoid arthritis fibroblast-like synovial cells (RA-FLS) (Articular Engineering, Northbrook, IL) are cocultured with *in vitro* differentiated T_h17/T_h1 cells to mimic inflammatory environment of synovial joint in RA patients, where TNF and IL-17A produced by activated T_h17/T_h1 cells drives the cytokines and chemokines production from RA-FLS. To evaluate the ability of JNJ-8104 to neutralize inflammatory responses mediated by endogenous TNF and IL-17A, various doses of JNJ-8104, CNTO 9809 (parental anti-TNF), CNTO 4782 (parental anti-IL-17A) and equal-molar fixed-ratio combination of CNTO 9809 and CNTO 4782 are incubated with coculture for 48 hours. IL-6 and GROα concentrations in the supernatants were measured using ELISA following manufacturer's instructions (R&D Systems, Minneapolis, MN).

JNJ-8104 activity in a mouse lung neutrophilia model

Pulmonary neutrophilia was induced by intranasal instillation of 0.3 ug in 50 µL volume purified recombinant human TNF and IL-17A in Balb/c mice. After 6 h, their lungs were lavaged with 2 volumes of 0.5 mL PBS containing 0.1% BSA and the total numbers of cells in BAL were counted by Advia system (Advia Hematology System, Bayer Corporation, Tarrytown, NY). To assess neutrophils influx, cytospin smears (Cytospin cytocentrifuge (Shandon, Pittsburgh, PA)) were stained with Hemacolor® Rapid staining of blood smear (Millipore Sigma, Danvers, MA) and 200 cells were counted under light microscope. To examine the effect of JNJ-8104 or its parental antibodies (CNTO 9809 and CNTO 4782) mice were dosed intraperitoneally with the test mAbs 18 hours prior to the instillation of cytokines. Control animals received isotype control in a similar fashion.

Cynomolgus monkey study design and sample collection

Cyno studies were conducted to characterize the PK and TNF/IL-17A TE for JNJ-8104 and its parental antibodies. The studies were conducted at Charles River Labs (CRL, Reno, NV), using biologics-naïve monkeys. All studies were approved by the Institutional Animal Care and Use Committee, and were performed in compliance with the Animal Welfare Act, the Guide for the Care and Use of Laboratory Animals and the Office of Laboratory Animal welfare.

In the main PK/TE study, the animals were divided into six groups (N =4/group). On Study Day 0, each animal received a single IV bolus dose of either JNJ-8104 (Duobody) at 0.3, 1 or 10 mg/kg, golimumab (anti-TNF parental antibody) at 0.15 or 0.5 mg/kg, or CNTO 6785 (bivalent anti-IL-17A antibody, which shares the same CDR as JNJ-8104) at 0.15 mg/kg. Blood samples

were collected at selected time points for PK and TNF/IL-17A TE measurements. Similarly, PK and TE samples were also collected from two cyno 3-month toxicology studies where the animals received 14 weekly IV doses on Days 1, 8, 15, 22, 29, 36, 43, 50, 57, 64, 71, 78, 85 and 92, respectively, of either golimumab at 50 mg/kg (N =10), golimumab and CNTO 6785 both at 50 mg/kg (N =4), or JNJ-8104 at 100 mg/kg (N =3).

First-in-human study in normal healthy subjects

The safety, tolerability, PK, PD and immunogenicity of JNJ-8104 were investigated in an FIH study (NCT02758392). Fifty-four healthy subjects were enrolled in one of five single IV dose levels (0.1, 0.3, 1, 3 and 10 mg/kg) or a single SC dose (1 mg/kg). Nine subjects were enrolled in each cohort: six active and three placebo per cohort. Blood samples were collected prior to study agent administration, and at 1, 4, 12, 24, 48, 72 and 96 hours after infusion, and 1, 2, 3, 4, 6, 8, 12 and 16 weeks after, to measure JNJ-8104 PK, total TNF and total IL-17A. The details of this FIH study were previously described.[26]

Bioanalytical methods

The concentrations of total JNJ-8104 in cyno serum were determined by a qualified electrochemiluminescent immunoassay (ECLIA) utilizing the MesoScale Discovery (MSD) platform. Briefly, after blocking, JNJ-8104 was captured by a biotinylated anti-human IgG antibody R10Z8E9 (Abcam, Cambridge, MA) onto a streptavidin-coated MSD plate. After incubation and washing, bound JNJ-8104 was detected by R10Z8E9 labeled with ruthenium. The assay was demonstrated to measure total JNJ-8104 and the presence of TNF or IL-17A did not affect the recovery. Serum concentrations of JNJ-8104 in human serum were determined using a validated ECLIA method as described previously.[26]

Golimumab concentrations in cyno serum were determined by a validated ECLIA using a biotinylated anti-idiotypic antibody for capture and another Sulfo-Tag anti-idiotypic antibody for detection. CNTO 6785 concentrations in cyno serum were determined by a validated ECLIA using another pair of anti-idiotypic antibodies against CNTO 6785, a biotinylated anti-idiotypic antibody for capture and a ruthenium-labeled anti-idiotypic antibody for detection. The anti-idiotypic antibodies used for golimumab and CNTO 6785 measurements were all produced by Janssen R&D.

The total TNF concentrations in cyno and human serum were measured with qualified ECLIAs on the MSD platform. In short, a non-competing biotinylated mouse anti-monkey TNF antibody (Clone QS-Tc, Cell Sciences) was immobilized on an MSD GOLD 96-Well Streptavidin Plate. Sample was introduced and incubated. After washing, a non-competing ruthenium-labeled chimeric anti-human TNF antibody (CNTO 3514, Janssen R&D) was added. Total TNF concentrations are determined by interpolation from the standard curve using a 5PL curve fit, with $1/y^2$ weighting (WatsonLIMS). While the human and cyno assays shared similar procedures, the assays were qualified specifically for each species separately.

The concentrations of total IL-17A in cyno and human serum were measured with similar MSD assays, except using a non-competing biotinylated mouse anti-human IL-17A antibody (Clone 4H1524.1, Rockland) for capture and a non-competing ruthenium-labeled mouse IgG1 anti-human IL-17A antibody (Clone 41802, R&D Systems) for detection. Total IL-17A concentrations are determined by interpolation from the standard curve using a 5PL curve fit, with $1/y^2$ weighting (WatsonLIMS). While the human and cyno assays shared similar procedures, the assays were qualified specifically for each species separately. The free (i.e., not bound to drug) IL-17A concentrations in cyno serum were measured by first passing the samples through a Protein G column (Pierce Biotechnology, Rockford, Illinois, USA), and then detected by Singulex Erenna platform (Millipore Sigma, Burlington, MA, USA). The rest of the assay follows the same procedure as the total IL-17A assay.

The free (i.e., not bound to drug) TNF concentrations in cyno serum were also measured with a qualified assay on the Singulex Erenna platform. Given the low baseline concentrations of TNF in normal cyno serum, no meaningful-free TNF concentrations were obtained following JNJ-8104 dosing.

PK/TE model

A quasi-equilibrium TMDD model[50] was used to describe the interaction between the antibodies and their targets in the systemic circulation of cynos. The model scheme is shown in Figure 4a. In this model, the two target-binding arms of a mAb were assumed to bind their targets independently, i.e., for golimumab and CNTO 6785, each drug molecule was treated as containing two independent target-binding sites for TNF and IL-17A, respectively; and for JNJ-8104, each drug molecule contains one target-binding site for TNF and one for IL-17A. The simplification of the TMDD model replaces the two *in vivo* binding constants (k_{on} and k_{off}), which are difficult to estimate, with one equilibrium dissociation constant (K_D):

$$K_D = R_{free} \cdot C_{free}/RC \tag{2}$$

where C_{free} represents the free drug concentration, R_{free} represents the free target concentration and RC represents the drug-target complex concentration. Rearrangement of Equation (2) leads to:

$$\begin{aligned} R_{free} = {}^1\!/_2 \cdot \{ & -(C_{tot} - R_{tot} + K_D) \\ & + SQRT\left((C_{tot} - R_{tot} + K_D)^2\right. \\ & \left. +4 \cdot K_D \cdot R_{tot}\right)\} \end{aligned} \tag{3}$$

where C_{tot} represents the total drug concentration and R_{tot} represents the total target concentration.[29,30] Importantly, Equation (3) shows that the free target level under 'quasi-equilibrium' conditions is a function of total drug level, total target level, and *in vivo* K_D.

Other parameters in Figure 4A include V_1 and V_2, volumes of distribution in the central and peripheral compartments, respectively; Q, distributional clearance between central and peripheral compartments; k_{el_drug}, first-order elimination rate constant of free drug; k_{syn}, zero-order target synthesis rate constant; k_{deg}, first-order free target degradation rate constant; $k_{el\_complex}$, first-order elimination rate constant of the drug-target complex.

Predicting JNJ-8104 human PK and TE based on cyno data

The PK/TE modeling results for JNJ-8104 were used to predict TNF and IL-17A target engagement following JNJ-8104 dosing in humans, using allometric scaling with fixed exponents for volumes of distribution (V) and clearance (CL), assuming 70 kg human body weight (BW) and 3.0 kg cyno BW. CL (CL = k_{el_drug} * V_1) and Q were scaled using an exponent value of 0.85, V_1 and V_2 were scaled using an exponent value of 1.[51] The human k_{deg} and $k_{el\_complex}$ values were scaled using an exponent value of −0.25 based on the estimated values in cynos for each target.[51] The apparent *in vivo* K_D values for TNF and IL-17A were assumed to be the same as the PK/TE model-estimated values from cynos.

The human serum TNF and IL-17A assays employed in this study had an LLOQ at 10 pg/mL; the baseline levels of TNF and IL-17A were below this limit in all normal human subjects in the JNJ-8104 FIH study.[26] A wide range of human serum baseline levels of TNF has been reported.[40] A baseline level of human TNF at 0.9 pg/mL was used for modeling purpose based on the reported population median value for TNF baseline in RA patients,[40] and it is consistent with the observed mean TNF baseline in normal cynos (0.6 pg/mL). The human serum IL-17A baseline was assumed to be 1.365 pg/mL for simulation purpose based on observed mean IL-17A baseline in normal cynos in studies described earlier.

Acknowledgments

The authors would like to thank Gopi Shankar (Janssen R&D) for thoroughly reviewing this manuscript. The authors would also like to acknowledge Xi Chen and Lanyi Xie for contributions to the initial project, Thai Dinh, Eilyn Lacy, Donald Heald, Xirong Zheng, Nando Bansal and Jennifer Nemeth-Seay (Janssen R&D) for their scientific input of this manuscript.

References

1. Kotsovilis S, Andreakos E. Therapeutic human monoclonal antibodies in inflammatory diseases. Methods Mol Biol. 2014;1060:37–59.
2. Lai Y, Dong C. Therapeutic antibodies that target inflammatory cytokines in autoimmune diseases. Int Immunol. 2016;28 (4):181–88. doi:10.1093/intimm/dxv063.
3. Siebert S, Tsoukas A, Robertson J, McInnes I, Touyz RM. Cytokines as therapeutic targets in rheumatoid arthritis and other inflammatory diseases. Pharmacol Rev. 2015;67(2):280–309. doi:10.1124/pr.114.009639.
4. Fischer JA, Hueber AJ, Wilson S, Galm M, Baum W, Kitson C, Auer J, Lorenz SH, Moelleken J, Bader M, et al. Combined inhibition of tumor necrosis factor α and interleukin-17 as a therapeutic opportunity in rheumatoid arthritis: development and characterization of a novel bispecific antibody. Arthritis Rheumatol. 2015;67 (1):51–62. doi:10.1002/art.38896.
5. Campbell J, Lowe D, Sleeman MA. Developing the next generation of monoclonal antibodies for the treatment of rheumatoid arthritis. Br J Pharmacol. 2011;162(7):1470–84. doi:10.1111/j.1476-5381.2010.01183.x.
6. McInnes IB, Buckley CD, Isaacs JD. Cytokines in rheumatoid arthritis — shaping the immunological landscape. Nat Rev Rheumatol. 2016;12(1):63–68. doi:10.1038/nrrheum.2015.171.
7. Buckland J. Anti-TNF and anti-IL-17 antibodies—better together! Nat Rev Rheumatol. 2014;10(12):699. doi:10.1038/nrrheum.2014.183.
8. Alzabin S, Abraham SM, Taher TE, Palfreeman A, Hull D, McNamee K, Jawad A, Pathan E, Kinderlerer A, Taylor PC, et al. Incomplete response of inflammatory arthritis to TNFα blockade is associated with the Th17 pathway. Ann Rheum Dis. 2012;71 (10):1741–48. doi:10.1136/annrheumdis-2011-201024.
9. Wajant H, Pfizenmaier K, Scheurich P. Tumor necrosis factor signaling. Cell Death Differ. 2003;10:45–65.
10. Kalliolias GD, Ivashkiv LB. TNF biology, pathogenic mechanisms and emerging therapeutic strategies. Nat Rev Rheumatol. 2016;12 (1):49–62. doi:10.1038/nrrheum.2015.169.
11. Grell M, Wajant H, Zimmermann G, Scheurich P. The type 1 receptor (CD120a) is the high-affinity receptor for soluble tumor necrosis factor. Proc Natl Acad Sci U S A. 1998;95(2):570–75. doi:10.1073/pnas.95.2.570.
12. Parameswaran N, Patial S. Tumor necrosis factor-α signaling in macrophages. Crit Rev Eukaryot Gene Expr. 2010;20(2):87–103. doi:10.1615/CritRevEukarGeneExpr.v20.i2.10.
13. Chaabo K, Kirkham B. Rheumatoid arthritis — anti-TNF. Int Immunopharmacol. 2015;27(2):180–84. doi:10.1016/j.intimp.2015.04.051.
14. Kolls JK, Linden A. Interleukin-17 family members and inflammation. Immunity. 2004;21(4):467–76. doi:10.1016/j.immuni.2004.08.018.
15. Miossec P, Kolls JK. Targeting IL-17 and TH17 cells in chronic inflammation. Nat Rev Drug Discov. 2012;11(10):763–76. doi:10.1038/nrd3794.
16. van den Berg WB, Miossec P. IL-17 as a future therapeutic target for rheumatoid arthritis. Nat Rev Rheumatol. 2009;5(10):549–53. doi:10.1038/nrrheum.2009.179.
17. Kurschus FC, Moos S. IL-17 for therapy. J Dermatol Sci. 2017;87 (3):221–27. doi:10.1016/j.jdermsci.2017.06.010.
18. McInnes IB, Mease PJ, Kirkham B, Kavanaugh A, Ritchlin CT, Rahman P, van der Heijde D, Landewé R, Conaghan PG, Gottlieb AB, et al. Secukinumab, a human anti-interleukin-17A monoclonal antibody, in patients with psoriatic arthritis (FUTURE 2): a randomised, double-blind, placebo-controlled, phase 3 trial. Lancet. 2015;386(9999):1137–46. doi:10.1016/S0140-6736(15)61134-5.
19. Moran EM, Mullan R, McCormick J, Connolly M, Sullivan O, Fitzgerald O, Bresnihan B, Veale DJ, Fearon U. Human rheumatoid arthritis tissue production of IL-17A drives matrix and cartilage degradation: synergy with tumour necrosis factor-α, oncostatin M and response to biologic therapies. Arthritis Res Ther. 2009;11(4):R113. doi:10.1186/ar2772.
20. Koenders MI, Marijnissen RJ, Devesa I, Lubberts E, Joosten LA, Roth J, van Lent PLEM, van de Loo FA, van den Berg WB. Tumor necrosis factor-interleukin-17 interplay induces S100A8, interleukin-1β, and matrix metalloproteinases, and drives irreversible cartilage destruction in murine arthritis: rationale for combination treatment during arthritis. Arthritis Rheum. 2011;63(8):2329–39. doi:10.1002/art.30418.
21. Shen F, Verma AH, Volk A, Jones B, Coleman BM, Loza MJ, et al. Combined blockade of TNF-α and IL-17A alleviates progression of collagen-induced arthritis without causing serious infections in mice. J Immunol (Baltimore, Md : 1950). 2019;202(7):2017–26.
22. Kirkham BW, Lassere MN, Edmonds JP, Juhasz KM, Bird PA, Lee CS, Shnier R, Portek IJ. Synovial membrane cytokine expression is predictive of joint damage progression in rheumatoid arthritis: a two-year prospective study (the DAMAGE study cohort). Arthritis Rheum. 2006;54(4):1122–31. doi:10.1002/art.21749.
23. Khatri A, Goss S, Jiang P, Mansikka H, Othman AA. Pharmacokinetics of ABT-122, a TNF-α- and IL-17A-targeted dual-variable domain immunoglobulin, in healthy subjects and patients with rheumatoid arthritis: results from three Phase I trials. Clin Pharmacokinet. 2018;57(5):613–23. doi:10.1007/s40262-017-0580-y.
24. Genovese MC, Weinblatt ME, Aelion JA, Mansikka HT, Peloso PM, Chen K, Li Y, Othman AA, Khatri A, Khan NS, et al. ABT-122, a bispecific dual variable domain immunoglobulin targeting tumor necrosis factor and interleukin-17A, in patients with rheumatoid arthritis with an inadequate response to methotrexate:

a randomized, double-blind study. Arthritis Rheumatol. 2018;70 (11):1710–20. doi:10.1002/art.40580.
25. Silacci M, Lembke W, Woods R, Attinger-Toller I, Baenziger-Tobler N, Batey S, Santimaria R, von der Bey U, Koenig-Friedrich S, Zha W, et al. Discovery and characterization of COVA322, a clinical-stage bispecific TNF/IL-17A inhibitor for the treatment of inflammatory diseases. MAbs. 2016;8(1):141–49. doi:10.1080/19420862.2015.1093266.
26. Akpalu DE, Frederick B, Nnane IP, Yao Z, Shen F, Ort T, Fink D, Dogmanits S, Raible D, Sharma A, et al. Pharmacokinetics, pharmacodynamics, immunogenicity, safety, and tolerability of JNJ-61178104, a novel tumor necrosis factor-alpha and interleukin-17A bispecific antibody, in healthy subjects. J Clin Pharmacol. 2019;59(7):968–78. doi:10.1002/jcph.1393.
27. Davda JP, Hansen RJ. Properties of a general PK/PD model of antibody-ligand interactions for therapeutic antibodies that bind to soluble endogenous targets. MAbs. 2010;2(5):576–88. doi:10.4161/mabs.2.5.12833.
28. Zheng S, McIntosh T, Wang W. Utility of free and total target measurements as target engagement and efficacy biomarkers in biotherapeutic development-opportunities and challenges. J Clin Pharmacol. 2015;55(Suppl S3):S75–S84. doi:10.1002/jcph.357.
29. Lee JW, Kelley M, King LE, Yang J, Salimi-Moosavi H, Tang MT, Lu J-F, Kamerud J, Ahene A, Myler H, et al. Bioanalytical approaches to quantify "total" and "free" therapeutic antibodies and their targets: technical challenges and PK/PD applications over the course of drug development. Aaps J. 2011;13(1):99–110. doi:10.1208/s12248-011-9251-3.
30. Wang W, Wang X, Doddareddy R, Fink D, McIntosh T, Davis HM, Zhou H. Mechanistic pharmacokinetic/target engagement/pharmacodynamic (PK/TE/PD) modeling in deciphering interplay between a monoclonal antibody and its soluble target in cynomolgus monkeys. Aaps J. 2014;16(1):129–39. doi:10.1208/s12248-013-9545-8.
31. Agoram BM, Martin SW, van der Graaf PH. The role of mechanism-based pharmacokinetic–pharmacodynamic (PK–PD) modelling in translational research of biologics. Drug Discov Today. 2007;12(23–24):1018–24. doi:10.1016/j.drudis.2007.10.002.
32. Danhof M, de Lange EC, Della Pasqua OE, Ploeger BA, Voskuyl RA. Mechanism-based pharmacokinetic-pharmacodynamic (PK-PD) modeling in translational drug research. Trends Pharmacol Sci. 2008;29(4):186–91. doi:10.1016/j.tips.2008.01.007.
33. Betts AM, Clark TH, Yang J, Treadway JL, Li M, Giovanelli MA, Abdiche Y, Stone DM, Paralkar VM. The application of target information and preclinical pharmacokinetic/pharmacodynamic modeling in predicting clinical doses of a Dickkopf-1 antibody for osteoporosis. J Pharmacol Exp Ther. 2010;333(1):2–13. doi:10.1124/jpet.109.164129.
34. Ait-Oudhia S, Lowe PJ, Mager DE. Bridging clinical outcomes of canakinumab treatment in patients with rheumatoid arthritis with a population model of IL-1β kinetics. CPT Pharmacometrics Syst Pharmacol. 2012;1(9):e5. doi:10.1038/psp.2012.6.
35. Chen X, Jiang X, Jusko WJ, Zhou H, Wang W. Minimal physiologically-based pharmacokinetic (mPBPK) model for a monoclonal antibody against interleukin-6 in mice with collagen-induced arthritis. J Pharmacokinet Pharmacodyn. 2016;43(3):291–304. doi:10.1007/s10928-016-9472-2.
36. Chen X, Jiang X, Doddareddy R, Geist B, McIntosh T, Jusko WJ, Zhou H, Wang W. Development and translational application of a minimal physiologically based pharmacokinetic model for a monoclonal antibody against interleukin 23 (IL-23) in IL-23-induced psoriasis-like mice. J Pharmacol Exp Ther. 2018;365 (1):140–55. doi:10.1124/jpet.117.244855.
37. Reid J, Zamuner S, Edwards K, Rumley S-A, Nevin K, Feeney M, Zecchin C, Fernando D, Wisniacki N. In vivo affinity and target engagement in skin and blood in a first-time-in-human study of an anti-oncostatin M monoclonal antibody. Br J Clin Pharmacol. 2018;84(10):2280–91. doi:10.1111/bcp.13669.
38. Wang W, Leu J, Watson R, Xu Z, Zhou H. Investigation of the mechanism of therapeutic protein-drug interaction between methotrexate and golimumab, an anti-TNFα monoclonal antibody. Aaps J. 2018;20(3):63. doi:10.1208/s12248-018-0219-4.
39. Takeuchi T, Miyasaka N, Tatsuki Y, Yano T, Yoshinari T, Abe T, Koike T. Baseline tumour necrosis factor alpha levels predict the necessity for dose escalation of infliximab therapy in patients with rheumatoid arthritis. Ann Rheum Dis. 2011;70(7):1208–15. doi:10.1136/ard.2011.153023.
40. Lazarus MN, Turner-Stokes T, Chavele K-M, Isenberg DA, Ehrenstein MR. B-cell numbers and phenotype at clinical relapse following rituximab therapy differ in SLE patients according to anti-dsDNA antibody levels. Rheumatology (Oxford). 2012;51 (7):1208–15. doi:10.1093/rheumatology/ker526.
41. Kaymakcalan Z, Sakorafas P, Bose S, Scesney S, Xiong L, Hanzatian DK, Salfeld J, Sasso EH. Comparisons of affinities, avidities, and complement activation of adalimumab, infliximab, and etanercept in binding to soluble and membrane tumor necrosis factor. Clin Immunol. 2009;131(2):308–16. doi:10.1016/j.clim.2009.01.002.
42. Ferraiolo BL, McCabe J, Hollenbach S, Hultgren B, Pitti R, Wilking H. Pharmacokinetics of recombinant human tumor necrosis factor-alpha in rats. Effects of size and number of doses and nephrectomy. Drug Metab Dispos. 1989;17:369–72.
43. Chen X, DuBois DC, Almon RR, Jusko WJ. Characterization and interspecies scaling of rhTNF-α pharmacokinetics with minimal physiologically based pharmacokinetic models. Drug Metab Dispos. 2017;45(7):798–806. doi:10.1124/dmd.116.074799.
44. Cowan J, Pandey S, Filion LG, Angel JB, Kumar A, Cameron DW. Comparison of interferon-γ-, interleukin (IL)-17- and IL-22-expressing CD4 T cells, IL-22-expressing granulocytes and proinflammatory cytokines during latent and active tuberculosis infection. Clin Exp Immunol. 2012;167(2):317–29. doi:10.1111/j.1365-2249.2011.04520.x.
45. Khatri A, Klunder B, Peloso PM, Othman AA. Exposure–response analyses demonstrate no evidence of interleukin 17A contribution to efficacy of ABT-122 in rheumatoid or psoriatic arthritis. Rheumatology (Oxford). 2019;58(2):352–60. doi:10.1093/rheumatology/key312.
46. Shealy DJ, Cai A, Staquet K, Baker A, Lacy ER, Johns L, Vafa O, Gunn G, Tam S, Sague S, et al. Characterization of golimumab, a human monoclonal antibody specific for human tumor necrosis factor α. MAbs. 2010;2(4):428–39. doi:10.4161/mabs.12304.
47. Eich A, Urban V, Jutel M, Vlcek J, Shim JJ, Trofimov VI, Liam C-K, Kuo P-H, Hou Y, Xiao J, et al. A randomized, placebo-controlled Phase 2 trial of CNTO 6785 in chronic obstructive pulmonary disease. COPD. 2017;14(5):476–83. doi:10.1080/15412555.2017.1335697.
48. Labrijn AF, Meesters JI, de Goeij BE, van den Bremer ET, Neijssen J, van Kampen MD, Strumane K, Verploegen S, Kundu A, Gramer MJ, et al. Efficient generation of stable bispecific IgG1 by controlled Fab-arm exchange. Proc Natl Acad Sci U S A. 2013;110(13):5145–50. doi:10.1073/pnas.1220145110.
49. Katsamba PS, Navratilova I, Calderon-Cacia M, Fan L, Thornton K, Zhu M, Bos TV, Forte C, Friend D, Laird-Offringa I, et al. Kinetic analysis of a high-affinity antibody/antigen interaction performed by multiple Biacore users. Anal Biochem. 2006;352 (2):208–21. doi:10.1016/j.ab.2006.01.034.
50. Mager DE, Krzyzanski W. Quasi-equilibrium pharmacokinetic model for drugs exhibiting target-mediated drug disposition. Pharm Res. 2005;22(10):1589–96. doi:10.1007/s11095-005-6650-0.
51. Deng R, Iyer S, Theil F-P, Mortensen DL, Fielder PJ, Prabhu S. Projecting human pharmacokinetics of therapeutic antibodies from nonclinical data: what have we learned? MAbs. 2011;3 (1):61–66. doi:10.4161/mabs.3.1.13799.